

Interaction between the Fermi-edge singularity and optical phonons in $\text{Al}_x\text{Ga}_{1-x}\text{As}/\text{In}_y\text{Ga}_{1-y}\text{As}/\text{GaAs}$ heterostructures

Yu. I. Mazur,* G. G. Tarasov,† Z. Ya. Zhuchenko,† H. Kissel,‡ U. Müller, Vas. P. Kunets, and W. T. Masselink§
Department of Physics, Humboldt-Universität zu Berlin, Invalidenstrasse 110, D-10115 Berlin, Germany

(Received 29 November 2001; revised manuscript received 5 February 2002; published 9 July 2002)

Many-electron effects in pseudomorphically strained modulation-doped $\text{Al}_x\text{Ga}_{1-x}\text{As}/\text{In}_y\text{Ga}_{1-y}\text{As}/\text{GaAs}$ ($x=0.20$, $y=0.19$) heterostructures are investigated using photoluminescence as a function of magnetic field B , temperature T , and excitation density I . The interaction of the many-body exciton (Fermi-edge singularity) with the longitudinal-optical-phonon is observed. Both the Fermi-edge singularity and the enhancement of the exciton-longitudinal optical phonon interaction can be controlled by varying the magnetic field; the strengths of these two many-body effects change with filling factor. They are synchronous both with each other and with the resonance of the upper Landau level with the Fermi level. The strength of this phonon replica when the Fermi level is resonant with a Landau level is attributed to the magnetic-field-dependent screening properties of the two-dimensional electron gas in the quantum well.

DOI: 10.1103/PhysRevB.66.035308

PACS number(s): 78.55.Cr, 78.20.Ls, 73.40.Kp

I. INTRODUCTION

Modulation-doped quantum wells (QW's) afford a unique opportunity to gain deeper insight into the properties of a two-dimensional electron gas (2DEG) and, in particular, to its response on the external perturbation, a variety of final-state excitations, and the electron-electron interactions.¹⁻³ The optical properties are dominated by the Fermi-edge singularity (FES), a continuum resonance whose spectral shape is governed by the Coulomb interactions of the photoexcited carriers with the low-lying Fermi-sea excitations.⁴⁻⁶ In addition, lattice [longitudinal-optical (LO) phonons] and Fermi-sea (shake-up) excitations are observed in the magneto-optical spectra from QW's containing high densities of carriers.⁷⁻⁹ Usually the FES develops at the high-energy side of the photoluminescence (PL) band, whereas the LO phonons and shake-up excitations appear in the low-energy tail of the emission spectra.

The observation of the FES and other many-body effects such as shake-up satellites in magnetoluminescence spectra is associated with a strong hole localization.¹⁰ This localization energy has also recently been quantified.¹¹ The dependence of satellite intensity as a function of magnetic field is ascribed to the change of the Landau-level (LL) filling factor with field and to the resonant interaction between the LO-phonon and shake-up satellites. For even integer filling factors, the FES is found to be weak and the shake-up peaks relatively strong as a result of the poor screening of the electron-hole Coulomb interaction in the incompressible state of the 2DEG. Conversely, for odd integer filling factors, the FES strength is enhanced and the shake-up peaks become smeared into a continuous background due to efficient screening of the electron-hole interaction in the compressible state of the 2DEG.^{12,13}

This relatively simple picture is inconsistent with some recently reported behavior of LO-phonon sidebands (PSB's) in a magnetic field; these data may be interpreted as an indication that the strength of the LO PSB's accompanying the transitions between the electron and hole Landau levels

strongly depends not only on the strength of electron-LO-phonon (Fröhlich) coupling but also on the interference between electron-phonon and hole-phonon recombination channels.¹⁴ This interference leads to a suppression of direct-transition PSB's and to an inverted dependence in relative strength for indirect-transition PSB's compared with that of the zero-phonon lines. The physical mechanisms governing the optical processes with a 2DEG participation are not yet completely explored and details of the valence-band structure, the hole localization, and intersubband coupling need to be clarified.

It has been recently demonstrated that even in the presence of hole localization the QW system has to be slightly optically "heated," creating a small concentration of non-equilibrium holes, to develop the FES enhancement in the PL spectrum.¹⁵ The observed nonmonotonic temperature and excitation density dependencies of the FES suggest the need to reevaluate the picture based on weakly localized holes.¹⁶ In this paper, we present data describing the correlated behavior of the FES and its PSB in modulation-doped $\text{Al}_x\text{Ga}_{1-x}\text{As}/\text{In}_y\text{Ga}_{1-y}\text{As}/\text{GaAs}$ heterostructures which requires a refined description of the electron-phonon coupling in a dense 2DEG system with hole localization.

II. EXPERIMENTAL DETAILS

A series of pseudomorphic modulation-doped $\text{Al}_x\text{Ga}_{1-x}\text{As}/\text{In}_y\text{Ga}_{1-y}\text{As}/\text{GaAs}$ heterostructures were grown to allow the conditions of the FES and PSB observation. The epilayer sequence for the sample which is mainly described in this paper consists of a GaAs buffer layer, a 15-nm undoped $\text{In}_{0.19}\text{Ga}_{0.81}\text{As}$ strained QW (2DEG channel), a 7.5-nm $\text{Al}_{0.20}\text{Ga}_{0.80}\text{As}$ undoped spacer, a 35-nm $\text{Al}_{0.20}\text{Ga}_{0.80}\text{As}$ heavily Si-doped supplier layer with $N_D=2\times 10^{18}\text{ cm}^{-3}$, and a 5-nm Si-doped GaAs cap layer with $N_D=2.5\times 10^{18}\text{ cm}^{-3}$. The electron sheet density n_s of the 2D electrons, obtained from low-field Hall measurements down to 4.2 K is about $n_s=1.05\times 10^{12}\text{ cm}^{-2}$. Double-crystal x-ray-diffraction together with simulation were used to verify the samples' structural parameters. The x-ray data also indicate a

high quality of the structures under investigation.

The PL was excited by the 514.5-nm line of a cw Ar⁺ laser and was dispersed through a 3/4-m Czerny-Turner scanning spectrometer, with a spectral resolution better than 0.1 meV. The samples were mounted in an Oxford Spectromag 4000 system allowing measurements in magnetic fields up to 7 T and at temperatures from 1.7 to 300 K.

In order to identify weak peaks lying in close proximity to much stronger ones, the number and approximate energetic position of the peaks are located using the second derivative of the PL spectrum. The entire spectrum is then deconvoluted into a set of Gaussian-shaped curves with their maxima at the energies determined using the second derivative. The convolution of these Gaussians reproduces the spectral shape of the original PL signal. In this fashion the various contributions in the PL spectrum have been distinguished and analyzed, and, in particular, the integrated intensity of relatively weak features reliably determined.

III. RESULTS AND DISCUSSION

Figure 1 shows the PL behavior in a magnetic field. At zero magnetic field, the dominant feature results from the transition between the $n_e=1$ 2DEG state and the $n_h=1$ heavy-hole state. At low temperatures, this feature (E_{11}) is a relatively broad peak with its maximum at 1.2837 eV and a full width at half magnitude of 16 meV. A second peak E_{21} observed at 1.3249 eV is ascribed to the transition between the $n_e=2$ 2DEG state and the $n_h=1$ heavy-hole state. Identification of the photoluminescence peaks is aided by a self-consistent solution of the coupled Schrödinger and Poisson equations. The Fermi level for a given temperature has been calculated iteratively from the charge-neutrality condition. The intersubband separation $\Delta=E_2-E_1$ in the conduction band is found to be 45 meV, and E_F is 8 meV below the E_2 energy. To correctly model the overall PL line shape for non-zero temperatures, the technique of Lyo and Jones is used.¹⁷ Thus, differences in the electron and hole quasi-Fermi levels, level broadening due to ionized-impurity scattering of the majority and minority carriers, and impurity-assisted recombination are included. Higher excitation densities can also be modeled by adjusting the electron temperature (experimentally measured as a function of excitation intensity) and allowing the electron and hole densities to increase. When the temperature and/or excitation density is increased, the $n=2$ electron state becomes populated and the PL feature related to the $n=2$ state (E_{21} transition) is also measured.

A magnetic field applied perpendicular to the layer surface quantizes free electron and hole states into LL's. This quantization is reflected in the PL, which breaks up into a series of peaks corresponding to transitions between LL's of the electron conduction band and those of the heavy-hole valence band (light-hole states are separated by ~ 60 meV in these structures and are not taken into account in our study). Electron-hole recombination occurs between LL's with the same quantum numbers $N_e, N_h=0, 1, 2, \dots$ according to the well-known selection rule. Under low-level excitation and at low temperature, most of the photoexcited holes relax into the LL ground state, 0_h , and only the radiative

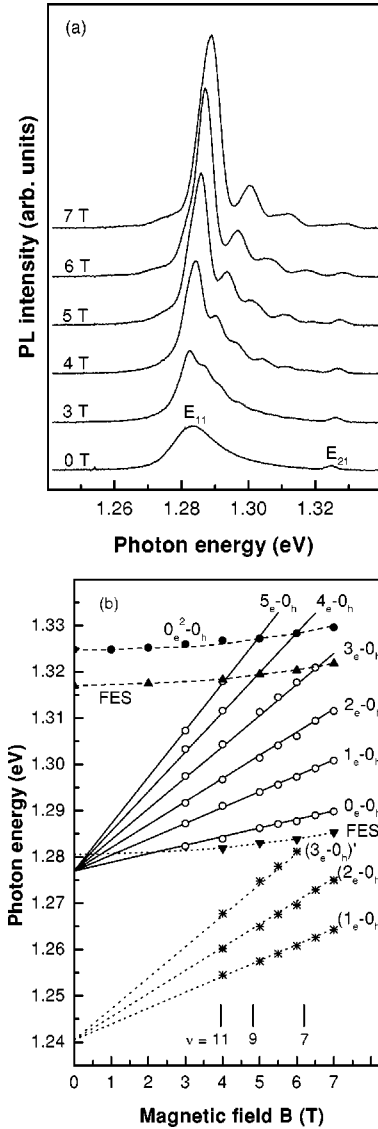


FIG. 1. (a) Magnetic-field-induced transformation of the PL spectrum at low temperature ($T=6$ K). The E_{11} and E_{21} transition energies at $B=0$ T are marked. (b) Landau-level fan plot. On the low-energy side of the PL spectra LO-phonon satellites of the $N_e \rightarrow 0_h$ ($N_e \geq 1$) transitions are observed. Vertical bars show the values of the filling factor ν .

transition with electrons in the 0_e state is allowed, the transitions with $N_e > 0$ being nominally forbidden. Due to carrier-impurity interactions these indirect transitions become allowed and are also seen in the magnetoluminescence.¹⁸ Electron-hole emission arising primarily from the direct $0_e \rightarrow 0_h$ transition is accompanied by emission from the nominally forbidden $1_e \rightarrow 0_h, 2_e \rightarrow 0_h, 3_e \rightarrow 0_h, \dots$ transitions, which have much weaker oscillator strengths in comparison with the allowed transitions ($N_e - N_h = 0$). The measured recombination energies of Landau levels with indices N_e and N_h and magnetic-field strength B are given by

$$E(N_e, N_h) = E_g^* + \hbar e B \left(\frac{1}{2\mu} + \frac{N_e}{m_e^*} + \frac{N_h}{m_h^*} \right), \quad (1)$$

where E_g^* is the effective energy gap; $E_{e1}-E_{hh1}$, m_e^* and m_h^* are the electron and hole effective masses; and μ is the reduced effective mass of the electron and hole. The number of LL's which are occupied for a given magnetic-field strength and Fermi energy is determined by the LL filling factor

$$\nu = \hbar n_s / eB = E_F / \hbar \omega_c, \quad (2)$$

where n_s is the 2DEG density and ω_c is the cyclotron frequency. For a given filling factor, ν , the maximum occupied Landau level when $N_h=0$ has an index N_e given by $N_e(\text{max})=(\nu-1)/2$. Using the n_s value derived above, it is straightforward to find that at $B=7$ T only LL's with $N_e=0, 1$, and 2 are filled resulting in three PL peaks visible in Fig. 1.

The transition energies derived from the PL spectra are plotted in Fig. 1(b) as a function of magnetic field. By fitting the LL fan plot [Fig. 1(b)] to Eq. 1, the effective energy gap, E_g^* , may be precisely determined. This value of E_g^* in the $\text{In}_{0.19}\text{Ga}_{0.81}\text{As}$ QW is found to be 1.2787 eV, significantly smaller than the value $E_{11}=1.2837$ eV, the maximum in the PL spectrum at $B=0$ T. The spectral blueshift of the PL onset observed experimentally is consistent with the theoretically predicted shift caused by the scattering of electrons (or holes) into virtual intermediate states before (after) the recombination.¹⁷ The impurity and alloy potential scattering within the $\text{In}_y\text{Ga}_{1-y}\text{As}$ layer, as well as the scattering by ionized donors on the other side of the spacer layer are primarily responsible for the broadening and spectral shift of the E_{11} transition. The energies of the various Landau levels as a function of magnetic field, furthermore, allow us to determine the electron effective mass, $m_e^*=0.0634$ (± 0.0003) m_0 and the hole effective mass, $m_h^*=0.091m_0$. The relatively small value for m_h^* is due to the strain-induced coupling between the heavy- and light-hole bands. The dependence of the E_{21} transition on magnetic field is also shown in Fig. 1(b) and is well approximated by a B^2 dependence typical for diamagnetic excitons.

Below the principal $0_e \rightarrow 0_h$ transition energy a series of phonon satellite lines is seen in the fan chart of Fig. 1(b). Each $N_e \rightarrow 0_h$ ($N_e \geq 1$) LL fan is replicated by a satellite. The phonon satellites arise from the LO-phonon Fröhlich interaction and occur to be intensive when the initial state of the PL includes a localized hole.¹⁹ The magnetic-field dependencies of the satellite energies converge onto the energy axis at $B=0$ T, giving the energy of 36.5 meV below E_g^* that corresponds to the GaAs-like LO-phonon energy. It is also notable that the FES feature is replicated also by the same phonon energy.

Displaying the magnetoluminescence on a semilogarithmic scale as in Fig. 2 and identifying the peak positions as described above using the second derivative and deconvolution techniques allows not only the various Landau levels to be identified, but also the FES and a number of phonon replicas. Figure 2 clearly shows the radiative transitions $N_e \rightarrow 0_h$ from LL's with $N_e \leq 3$ which are also the only electronic Landau levels expected to be populated at $B=5$ T based on the value of the filling factor [see Fig. 1(b)]. In

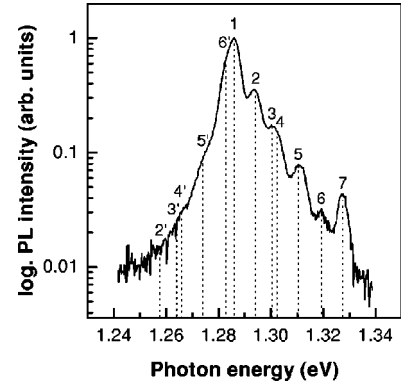


FIG. 2. Semilogarithmic representation of a magnetoluminescence spectrum with $B=5$ T and at $T=6$ K with a number of transitions identified. The labeling is as follows: 1— $0_e \rightarrow 0_h$ transition, 2— $1_e \rightarrow 0_h$ transition, 3— $1_e \rightarrow 1_h$ transition, 4— $2_e \rightarrow 0_h$ transition, 5— $3_e \rightarrow 0_h$ transition, 6—FES, and 7— $0_e^2 \rightarrow 0_h$ transition. The LO-phonon replicas of primary transitions are denoted as N' .

addition, the direct transition $1_e \rightarrow 1_h$ is revealed in the PL (feature 3 in Fig. 2) due to the energy distribution of holes in the valence band, which for low excitation density, is Boltzmann-like. The FES (feature 6 in Fig. 2) is identified first of all through its energetic dependence on magnetic field as seen in Fig. 1(b) and by comparing its zero-field energy with the self-consistent calculation. In addition, it becomes enhanced each time one of the successive LL's crosses the Fermi energy.

We have also investigated the dependence of the FES and the magnetoluminescence in general on temperature; the temperature-related changes of the PL spectrum at $B=7$ T are displayed in Fig. 3. First of all, one sees that the temperature dependence of diagonal and off-diagonal transitions

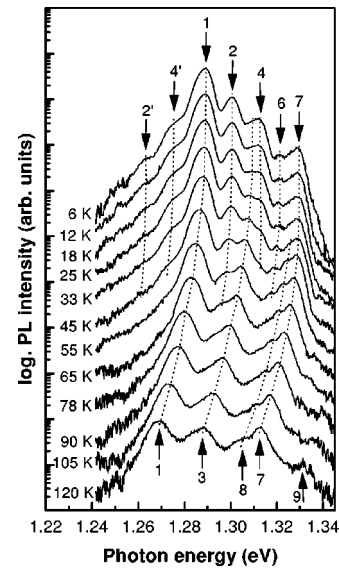


FIG. 3. Temperature-related evolution of the PL spectrum in magnetic field of $B=7$ T. Arrows mark the transitions as labeled in Fig. 2; additional peaks are 8— $2_e \rightarrow 2_h$ transition and 9—LL transitions related to the $n=2$ subband. The dashed lines are guides to assist in following the temperature development of the peaks.

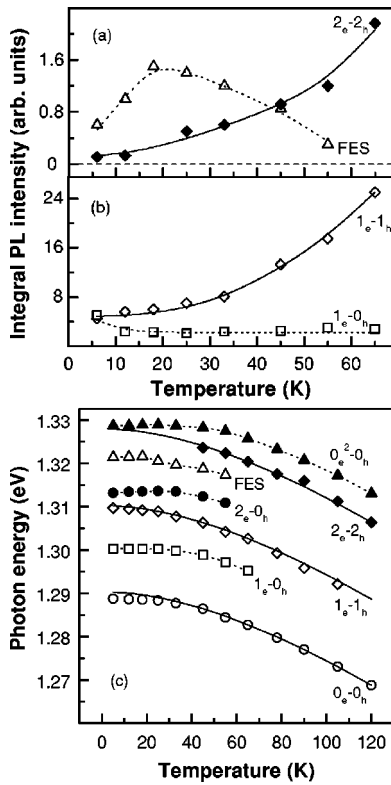


FIG. 4. Temperature dependence of the integral PL intensities for (a) FES and $2_e \rightarrow 2_h$, and (b) $1_e \rightarrow 1_h$ and $1_e \rightarrow 0_h$ transitions. (c) Temperature dependence of the inter-LL transition energies in the PL spectra at a magnetic field of $B = 7$ T. The solid lines show the temperature change of the band gap E_g .

between LL's is principally different. As the thermal population of higher hole LL's grows with increasing temperature, the allowed $1_e \rightarrow 1_h$ transition becomes relatively more intense at the expense of the nominally forbidden $N_e \rightarrow 0_h$ ($N_e \neq 0_e$) transitions.

It should be noted that the low-temperature ($T = 6$ K) spectrum between peaks 3 and 7 in Fig. 3 is dominated by the $1_e \rightarrow 1_h$, $2_e \rightarrow 0_h$, FES, and $0_e^2 \rightarrow 0_h$ transitions. At elevated temperature, however, the $2_e \rightarrow 2_h$ related feature develops at the low-energy side of the $0_e^2 \rightarrow 0_h$ transition, finally dominating the PL in this spectral range at temperatures above 45 K. Using the procedure of line-shape analysis described above, the different contributions for each temperature are identified. The temperature dependencies of their integral PL intensities are plotted in Figs. 4(a,b) and we see that the dependencies for the $1_e \rightarrow 1_h$ and $2_e \rightarrow 2_h$ transitions follow the thermal population of heavy-hole states. The integral intensity of the FES feature is seen to be a nonmonotonic function of temperature with a maximum intensity at $T \sim 18$ K, persisting up to 55 K, and then vanishing at still higher temperatures. The observed nonmonotonic dependence is not theoretically anticipated. It is expected that the FES feature will become less visible as the temperature is increased due to the smearing out of the Fermi surface and decays completely if the temperature reaches only $T \sim 10$ K. That is just contrary to what is observed experimentally. There are at least two mechanisms which could

lead to a thermally induced increase in FES intensity. One is that previous investigations of the FES in the pseudomorphically strained modulation-doped $\text{Al}_x\text{Ga}_{1-x}\text{As}/\text{In}_y\text{Ga}_{1-y}\text{As}/\text{GaAs}$ system have identified two hole localization energies.¹¹ Assuming that the higher-lying level (with higher hole binding energy) leads to a more-pronounced FES, a thermal activation of the lower-lying level could increase the population of the higher-lying level by bringing the populations closer to thermal equilibrium with each other. A second mechanism could be that acoustic phonons with $q = k_F$ aid in the development of the FES through their contribution to the multiple electron-hole scattering.

Figure 4(c) shows the temperature shift of the emission lines for the inter-LL transitions in a magnetic field of $B = 7$ T. The solid line shows the corresponding change of the band-gap energy. The total redshift of the entire spectrum is caused by the band-gap shrinkage, while the LL spacings remain intact. The well-pronounced deviation of the experimental points from the temperature dependence of the band gap for the $0_e \rightarrow 0_h$ transition can be attributed to fluctuations of the local potential energy in the QW.²⁰ These fluctuations also broaden the LL's. At low excitation densities and low temperature the photoexcited holes will populate predominantly the low-energy states within the broadened LL, and the transition energy becomes smaller than the gap between the corresponding electron and hole LL's. The width of the N th hole LL, Γ_N , is determined by both the magnitude of the fluctuations and their ranges. The magnetic length at $B = 7$ T is found to be of the same order as a characteristic scale of the potential fluctuations in our QW's. In this case Γ_N becomes smaller for larger N_h .²¹ Therefore the deviation from the E_g dependence at low temperature is expected to be smaller for larger N in accordance with the experiment. The temperature elevation results in a more regular distribution of holes over all states within broadened LL's and the inter-LL transition energies follow the temperature variation of E_g as one can see from Fig. 4(c). A similar effect is also expected for increasing excitation density.

Figure 5(a) shows the excitation density dependence of the low-temperature PL spectra ($T = 6$ K) in magnetic field $B = 7$ T. The dependence of the spectrum on excitation intensity is similar to that on temperature. It is clearly seen that the $1_e \rightarrow 1_h$ related feature increases in intensity at higher excitation densities. Nevertheless its appearance cannot be explained only by the subsequent filling of the hole LL. Butov *et al.*²⁰ have assumed that the "excess" recombination involving excited hole states can develop here due to an increase of the hole relaxation rate whenever the hole concentration is enlarged.

The behavior of the FES feature as a function of temperature and excitation density is of particular interest. Figure 5 depicts the FES development as a function of the excitation density at magnetic field of $B = 7$ T. It is clearly seen the FES feature increases in intensity with increasing excitation density as a distinct peak even if it was not detected at $B = 0$ T; the FES has its maximum intensity for an intensity of $I \approx I_0 = 2 \text{ W cm}^{-2}$ for lattice temperature $T_L = 6$ K and $B = 7$ T. At $I = I_0 = 20 \text{ W cm}^{-2}$ the FES feature coexists with the $n = 2$ conduction-band-heavy-hole transition, which

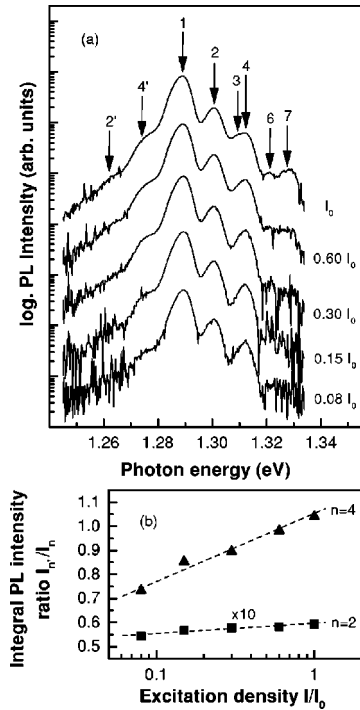


FIG. 5. (a) Excitation density-related evolution of the PL spectrum in magnetic field of $B=7$ T and at low temperature ($T=6$ K, $I_0=20$ W cm $^{-2}$). The labels have the same meaning as in Figs. 2 and 3. (b) Integral PL intensity ratio for LO satellites and parent LL transitions versus excitation density.

demonstrates the excitonlike behavior in a magnetic field [see Fig. 1(b)]. Figure 5 shows that whenever this transition appears, the FES feature repelled itself from the $n=2$ electronic state and moves towards lower energies against the Fermi energy. Increased excitation intensity results in a higher electron temperature; an analysis of the high-energy tail of the magnetoluminescence indicates that the electron temperature T_e is about 18 K for $I=I_0$ and already about 13 K for $I=0.1I_0$ when the lattice temperature $T_L=6$ K. Thus, one effect of the increased excitation energy is an increase in T_e . A second effect is a smearing of the Fermi edge due to excess hot electrons; this smearing, as long as it is not too great, can also aid in the development of the FES.

We now turn our attention to the peaks seen in Figs. 2, 3, and 5(a) with energy less than the $0_e \rightarrow 0_h$ transition which are due to longitudinal-optical-phonon replicas of other transitions and are seen only with applied magnetic field. These satellites result during the electron-hole recombination from the simultaneous emission of one GaAs-like LO phonon ($E_{ph}=36.5$ meV). The physical reasons for the appearance of phonon sidebands in a magnetic field have been widely discussed.^{10,14} The importance of hole localization as well as screening for the determination of the strength of the carrier-LO-phonon interaction has been demonstrated.^{10,22,23} So-called shake-up excitations¹⁰ are ruled out both because of the magnetic-field dependence and because they are typically only observed at rather high magnetic fields. The LO PSB's for transitions between the electron and hole LL's are found to be relatively strong and their strengths grow for larger N_e

values just in contrast with the relative strength of the zero-phonon lines. This dependence of the LO PSB strengths inverted by N_e has been explained by the suppression of small $\Delta N=|N_e-N_h|$ sidebands arising from the interference between the electron-phonon and hole-phonon recombination channels and the magnetic quantization in a 2D system.¹⁴ It is of interest that the observed PSB's are practically hidden in the noise if the excitation density is small enough and enhance significantly with increasing excitation density. Finally, they reach magnitudes comparable with those of the off-diagonal parent transitions. Figure 5(b) shows the dependencies of the integral intensities ratio for LO satellites and parent LL transitions on the excitation density. The integral intensities have been extracted from the PL spectra deconvolution following the procedure described above. The enhancement of the LO PSB's is also observed with increasing temperature. We consider the hole localization to be responsible in part for both the FES and PSB development. As mentioned above, the optical detection of quantum oscillations of the PL intensity in a magnetic field¹¹ revealed two sorts of holes in pseudomorphically strained modulation-doped $\text{Al}_x\text{Ga}_{1-x}\text{As}/\text{In}_y\text{Ga}_{1-y}\text{As}$ heterostructures: (i) nearly free, or in shallow traps, localized holes due to potential fluctuations, and (ii) those which are strongly localized by alloy fluctuations (with a localization energy of about 10 meV). The strong hole localization favors the strengthening of the electron-phonon coupling even in the case of a dense 2DEG, when it will be inevitably weakened due to screening. An analysis of Fig. 3 reveals that the FES decays at $T=55$ K and simultaneously the decay of accompanying PSB's takes place. As the temperature increases the Fermi edge is smeared out and the holes become delocalized. Both these factors tend to reduce the FES as well as the PSB strength. On the other hand the electron-phonon coupling can be also contributed by confined phonon modes and interface modes, which are expected to yield stronger PSB's. However, the contribution of these modes in layered alloy structures lacks a quantitative explanation at present.

Focusing on feature 6', just below the $0_e \rightarrow 0_h$ transition in energy, we note that it tracks feature 6, the FES, lying 36.5-meV lower in energy. That the energy dependence on magnetic field of feature 6' is the same as that of the FES, but one GaAs LO-phonon energy lower, is in marked contrast to the energetic dependence of the phonon replicas of Landau levels which track the parent Landau level as a function of magnetic field, and the shake-up excitations generally decrease in energy with increasing magnetic field. We identify feature 6' as the GaAs LO-phonon replica of the FES. It was noted above, in connection with the description of the magnetic-field behavior of the FES, that the integrated intensity of the FES increases when a Landau level crosses the Fermi level. This event occurs whenever the filling factor $\nu=2(\frac{1}{2}+N_e)$ for transitions with $N_h=0$, or for odd integer filling factors. When the Fermi level lies within the Landau level (which is broadened both by the spin splitting and by inhomogeneities in the electron's environment), a multiple electron-hole scattering across the Fermi level becomes more likely, favoring the FES enhancement. Such a behavior is

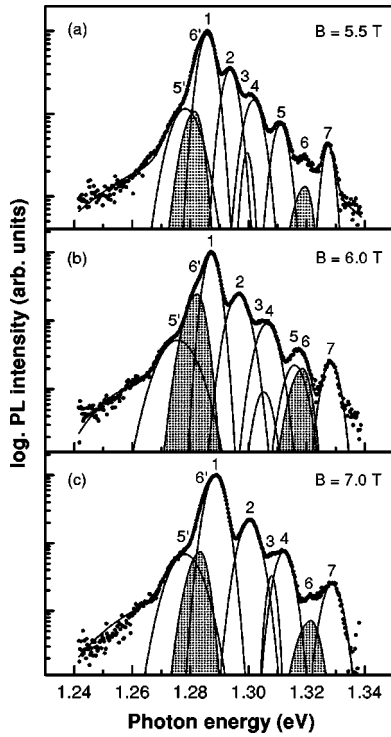


FIG. 6. The changes of the PL spectrum for magnetic-field strengths 5.5, 6.0, and 7.0 T at $T=6$ K. Shaded parts of the PL spectrum focus on the FES and its PSB.

opposite to that of shake-up excitations observed by Rubio *et al.*¹³ in the magneto-PL spectra of InGaAs/InP QW's. Their study of the joint evolution of FES and shake-up sidebands in a magnetic field shows that while the intensity of the FES is maximized for odd filling factors, that of the shake-up excitations is maximized for even filling factors, where the Fermi energy lies between two Landau levels. The shake-up excitations in this case are strong as a result of the poor screening of the electron-hole Coulomb interaction in the incompressible state of the electron gas.¹³

Figure 6 depicts this enhancement in the region of the Fermi level for three magnetic-field strengths between 5.5 and 7.0 T, specifically showing the results of line-shape spectral analysis of the PL spectra recorded at $B=5.5$, 6.0, and 7.0 T. For $B=5.5$ T, the filling factor ν takes the value $\nu=8$, indicating that the Fermi level lies between the (full) $N_e=3$ level and the (empty) $N_e=4$ level. One sees from Fig. 6 that the integrated intensity of the FES is relatively small. At $B=6$ T, the filling factor is $\nu=7.3$ and the LL with $N_e=3$ overlaps with the Fermi level. In this case, a notable enhancement of the FES is seen. Finally, at $B=7$ T the filling factor is $\nu=6.2$ and, again, the Fermi level lies between two LL's, in this case $N_e=2$ and $N_e=3$. As at $B=5.5$ T, the FES enhancement is again not very well pronounced. Returning to feature 6', the phonon replica of the FES, we see in Fig. 6 that its dependence of intensity on magnetic field is similar to that of the FES. The results of Fig. 6 are summarized in Fig. 7, which depicts the variation of integral PL intensity for the FES and its LO-phonon satellite with mag-

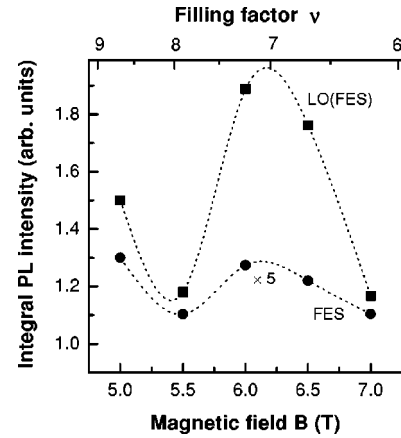


FIG. 7. Magnetic-field dependence of the integrated magnetoluminescence intensity as a function of magnetic field for the FES transition (filled circles) and its LO-phonon replica (filled squares).

netic field. The synchronous behavior of the intensities shows that both the FES and its phonon replica have maxima for odd filling factors and minima for even filling factors. Together with the energy dependence of the two peaks, these data definitively confirm the assignments of these two transitions. We believe this to be the first investigation of the coupling between the FES and phonons.

IV. CONCLUSIONS

To summarize, we have used magnetoluminescence to investigate many-body effects in a 2DEG in a pseudomorphically strained modulation-doped $\text{Al}_x\text{Ga}_{1-x}\text{As}/\text{In}_y\text{Ga}_{1-y}\text{As}$ heterostructure. The energies of the $N_e \rightarrow 0_n$ for $0 \leq N_e \leq 5$ and the $1_e \rightarrow 1_h$ Landau levels of the E_{11} transition were investigated as a function of magnetic field, temperature, and excitation intensity. In addition, many-body effects such as the FES and the coupling of the GaAs-like LO phonon to the Landau levels were investigated. We find that the FES is enhanced when the Fermi edge is somewhat smeared out, either thermally or due to nonequilibrium photoexcited electrons. Thus the FES has its maximum relative intensity at finite temperature and excitation intensity. A number of replicas of Landau-level transitions involving the GaAs-like LO phonon were also investigated. In addition, the LO-phonon replica of the FES was investigated. We demonstrate that its intensity also depends on the magnetic field as does the FES, being maximized when the Landau levels cross the Fermi level and minimized when the Fermi level is between two Landau levels. The strength of the phonon replica of the FES when the Fermi level is resonant with a Landau level is somewhat surprising considering the expected screening in this case, but is perhaps due to a reduction in screening in a magnetic field.

ACKNOWLEDGMENT

This work was supported by a NATO Linkage Grant.

- *Present address: Department of Physics, University of Arkansas, Fayetteville, AK 72701.
- †Also at Institute of Semiconductor Physics, National Academy of Sciences, Prospect Nauki 41, 03028 Kiev, Ukraine.
- ‡Present address: Ferdinand-Braun-Institut für Höchstfrequenztechnik, Albert-Einstein-Strasse 11, D-12489 Berlin, Germany.
- [§]Electronic address: massel@physik.hu-berlin.de
- ¹S. Schmitt-Rink, D.S. Chemla, and D.A.B. Miller, *Adv. Phys.* **38**, 89 (1989).
- ²M.S. Skolnick, K.J. Nash, M.K. Saker, and S.J. Bass, *Phys. Rev. B* **50**, 11 771 (1994).
- ³F.J. Rodríguez and C. Tejedor, *J. Phys.: Condens. Matter* **8**, 1713 (1996).
- ⁴M.S. Skolnick, J.M. Rorison, K.J. Nash, D.J. Mowbray, P.R. Tapster, S.J. Bass, and A.D. Pitt, *Phys. Rev. Lett.* **58**, 2130 (1987).
- ⁵W. Chen, M. Fritze, W. Walecki, A.V. Nurmikko, D. Ackley, J.M. Hong, and L.L. Chang, *Phys. Rev. B* **45**, 8464 (1992).
- ⁶T.V. Shahbazyan, N. Primožich, I.E. Perakis, and D.S. Chemla, *Phys. Rev. Lett.* **84**, 2006 (2000).
- ⁷K.J. Nash, M.S. Skolnick, M.K. Saker, and S.J. Bass, *Phys. Rev. Lett.* **70**, 3115 (1993).
- ⁸L.V. Butov, V.I. Grinev, V.D. Kulakovskii, and T.G. Andersson, *Phys. Rev. B* **46**, 13 627 (1992).
- ⁹P. Brockmann, J.F. Young, P. Hawrylak, and H.M. van Driel, *Phys. Rev. B* **48**, 11 423 (1993).
- ¹⁰M.S. Skolnick, D.J. Mowbray, D.M. Whittaker, and R.S. Smith, *Phys. Rev. B* **47**, 6823 (1993).
- ¹¹G.G. Tarasov, U. Müller, Yu.I. Mazur, H. Kissel, Z.Ya. Zhuchenko, C. Walther, and W.T. Masselink, *Phys. Rev. B* **58**, 4733 (1998).
- ¹²H.P. van der Meulen, J. Rubio, J.M. Calleja, H. Schweizer, F. Scholz, V. Härle, and R. Bergmann, *Surf. Sci.* **361/362**, 372 (1996).
- ¹³J. Rubio, H.P. van der Meulen, J.M. Calleja, V. Härle, R. Bergmann, and F. Scholz, *Phys. Rev. B* **55**, 16 390 (1997).
- ¹⁴S.K. Lyo, E.D. Jones, and J.F. Klem, *J. Phys.: Condens. Matter* **8**, L363 (1996).
- ¹⁵H. Kissel, U. Müller, C. Walther, W.T. Masselink, Yu.I. Mazur, G.G. Tarasov, G.Yu. Rud'ko, M.Ya. Valakh, V. Malyarchuk, and Z.Ya. Zhuchenko, *Phys. Rev. B* **61**, 8359 (2000).
- ¹⁶P. Hawrylak, N. Pulsford, and K. Ploog, *Phys. Rev. B* **46**, 15 193 (1992).
- ¹⁷S.K. Lyo and E.D. Jones, *Phys. Rev. B* **38**, 4113 (1988).
- ¹⁸S.K. Lyo, E.D. Jones, and J.F. Klem, *Phys. Rev. Lett.* **61**, 2265 (1988).
- ¹⁹M.S. Skolnick, K.J. Nash, P.R. Tapster, D.J. Mowbray, S.J. Bass, and A.D. Pitt, *Phys. Rev. B* **35**, 5925 (1987).
- ²⁰L.V. Butov, V.D. Kulakovskii, T.G. Andersson, and Z.G. Chen, *Phys. Rev. B* **42**, 9472 (1990).
- ²¹T. Ando, A. Fowler, and F. Stern, *Rev. Mod. Phys.* **54**, 437 (1982).
- ²²I. Brener, M. Olszakier, E. Cohen, E. Ehrenfreund, A. Ron, and L. Pfeiffer, *Phys. Rev. B* **46**, 7927 (1992).
- ²³L.V. Dao, M. Gal, G. Li, and C. Jagadish, *Appl. Phys. Lett.* **71**, 1849 (1997).